## Supplementary Materials

# Promoting effect of hydroxyl groups on the CO-SCR activity of Ir-Mo bimetallic catalysts under $O_2$ and $SO_2$

**Yixi Wang[1], Xiubiao Ma[1,2], Huixian Liu[3], Yujie Yuan[1,4], Yang Yang[1], Yaping Zhang[2], Wenqing Xu[1,*], Tingyu Zhu[1]**

[1]CAS Key Laboratory of Green Process and Engineering, Institute of Process Engineering, Chinese Academy of Sciences, Beijing 100190, China.
[2]Key Laboratory of Energy Thermal Conversion and Control, School of Energy and Environment, Southeast University, Nanjing 210096, Jiangsu, China.
[3]Beijing Municipal Research Institute of Eco-Environmental Protection, Beijing 100037, China.
[4]School of Chemistry and Chemical Engineering, North University of China, Taiyuan 030051, Shanxi, China.

[*]**Correspondence to:** Prof. Wenqing Xu, CAS Key Laboratory of Green Process and Engineering, Institute of Process Engineering, Chinese Academy of Sciences, Beijing 100190, China. E-mail: wqxu@ipe.ac.cn

Number of Pages: 16

Number of Texts: 2

Number of Figures: 9

Number of Tables: 2

## 1. Catalyst preparation

### Synthesis of Z5:

ZSM-5 zeolite was synthesized using tetrapropylammonium bromide (TPABr) as a structure-directing agent, silica sol as the silicon source, $NaAlO_2$ as the aluminum source, and NaOH as the base. NaOH (0.286 g) was dissolved in deionized water (20 g), followed by the addition of $NaAlO_2$ (0.327 g). The resulting solution (Solution A) was stirred for 1 h. Separately, NaOH (0.6 g) was dissolved in water (16 g), and TPABr (5.3 g) was added to the solution, which was stirred for 15 min. Silica sol (20 g) was then introduced into the mixture to form Solution B, followed by an additional 1 h of stirring. Solutions A and B were combined and stirred for 3 h. The final mixture was transferred into a 100 mL Teflon-lined stainless-steel autoclave and subjected to hydrothermal treatment at 170 °C for 32 h. The resulting solid was recovered by repeated centrifugation and washing, then dried at 100 °C. Finally, the dried powder was calcined in a muffle furnace at 550 °C for 6 h with a heating rate of 1 °C $min^{-1}$. The obtained ZSM-5 sample was labeled as Z5.

### Synthesis of Ir–Mo/Z5:

Z5 zeolite (1.90 g) was dispersed in deionized water (100 mL) under continuous stirring. Then, $H_2IrCl_6$ (1.95 mL) and ammonium molybdate (0.2576 g) were simultaneously added to the suspension. After stirring for 2 h, the mixture was subjected to rotary evaporation under reduced pressure at 60 °C and 80 rpm. The resulting solid residue was dried overnight in an oven at 100 °C. The dried powder was then calcined in air at 400 °C for 3 h with a heating rate of 10 °C $min^{-1}$ to obtain the Ir-Mo/Z5 catalyst.

**Synthesis of Ir–Mo@Z5:**

NaOH was dissolved in deionized water (0.286 g in 20 mL), followed by the addition of $NaAlO_2$ (0.327 g). The resulting solution (Solution A) was stirred for 1 h. Separately, another portion of NaOH (0.6 g) was added to water (16 mL), followed by TPABr (5.3 g), and stirred for 15 min. Silica sol (20 g) was then added, and the mixture (Solution B) was stirred for an additional 1 h. Meanwhile, $H_2IrCl_6$ (8.75 mL) and EDA (10 mL) were mixed and stirred for 30 min to form Solution C. Additionally, ammonium molybdate (0.8112 g) and TEPA (1.9 mL) were dissolved in water (11.35 mL) and stirred for 30 min to obtain Solution D. Solutions A, B, C, and D were then combined and stirred for 3 h. The final mixture was transferred into a 100 mL Teflon-lined stainless-steel autoclave and subjected to hydrothermal treatment at 170 °C for 32 h. The product was collected by centrifugation, washed repeatedly, and dried thoroughly at 100 °C. The dried solid was then calcined in a muffle furnace at 550 °C for 6 h with a heating rate of 1 °C $min^{-1}$ to obtain the Ir–Mo@Z5 catalyst. The schematic diagram of Ir-Mo@Z5 catalyst preparation is shown in **Supplementary Figure 1**.

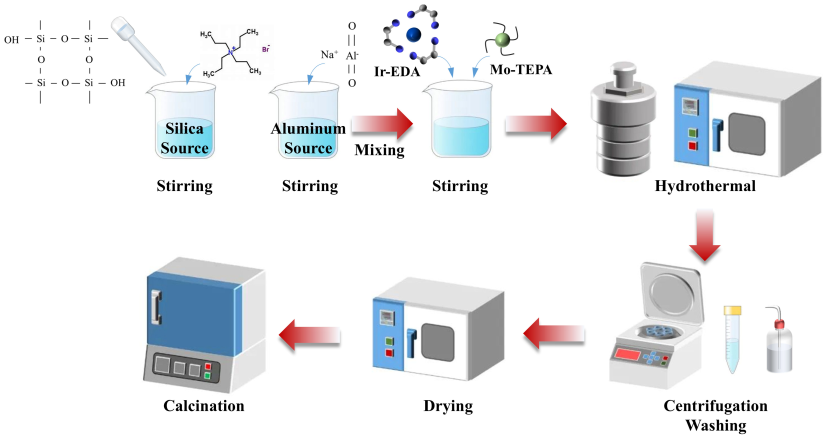

**Supplementary Figure 1. Schematic diagram of Ir-Mo@Z5 catalyst preparation.**

## 2. Catalyst characterization

(1) Brunauer–Emmett–Teller surface area analysis (BET)

Catalyst surface area was evaluated over the full relative pressure range at -196 °C using a NOVA 4000e analyzer. Before the sorption experiments, the samples underwent degassing at 300 °C for 2 hours. The specific surface areas were calculated using the Brunauer–Emmett–Teller (BET) method and the obtained isotherms.

(2) X–ray diffraction (XRD)

X–ray diffraction patterns of the synthesized sample powders were obtained using the X'Pert PRO MPD instrument with Cu Kα radiation operated at 40 kV and 40 mA. The diffraction data was collected over an angular range of 5° to 90° using a step size of 0.02°.

(3) Inductively coupled plasma optical emitting spectrometer (ICP–OES)

The elemental concentration of the sample was determined using an inductively coupled plasma optical emission spectrometer (ICP–OES) (Optima 5300DVk, PerkinElmer). The pre–treatment methods for the sample include microwave digestion (high–pressure and high–temperature treatment under acidic conditions) and alkaline dissolution. Microwave digestion is used to test the content of Ir, Al and Na in the sample, and alkaline dissolution is used to test the content of Si in the sample.

(4) Transmission electron microscopy (TEM)

The microstructures of different catalysts were analyzed employing a JEM–F200 field emission transmission electron microscope (TEM) and a JED–2300T energy spectrometer (EDS).

(5) High–angle annular dark–field scanning transmission electron microscopy (HAADF–STEM)

Atomic resolution high angle annular dark field scanning transmission electron microscopy (HAADF–STEM) images were acquired using a JEOL JEM–ARM200F STEM fitted with a CEOS probe and an image double spherical aberration corrector. The instrument has a guaranteed resolution of 0.08 nm. Before imaging, the dry samples were evenly dispersed on gold grids covered with a thin, holey carbon film.

(6) X–ray photoelectron spectroscopy (XPS)

X–ray photoelectron spectroscopy (XPS) was conducted using an AXIS Ultra instrument, with BE values calibrated by the C 1s peak at 284.8 eV.

(7) Temperature–programme reduction (TPR)

CO–temperature–programmed reduction (CO–TPR) experiments were carried out using a Hiden QGA mass spectrometer. For the CO–TPR experiment, 100 mg of Z5 and Ir/Z5 were pretreated with 20% $O_2/N_2$ (50 mL/min) at 400 °C for 30 minutes. Subsequently, 5% CO was introduced over the samples, and the temperature increase was recorded once the signal stabilized. The temperature was then increased from 50 to 800 °C at a rate of 10 °C per minute. The signals for $CO_2$ (m/z = 44) and $H_2$ (m/z = 2) were continuously monitored.

(8) Temperature–programmed desorption (TPD)

In the NO/$N_2O$/CO/$SO_2$-temperature-programmed desorption experiments (NO/ $N_2O$/CO/$SO_2$-TPD), 50 mg of the samples were exposed to 400 ppm NO/Ar, 200 ppm $N_2O$/Ar, 8000ppm CO/Ar or 200ppm $SO_2/N_2$ for 60 min at 50 °C and then blow with

Ar for 60 min. Finally, the temperature was raised to 800 °C in an Ar atmosphere at a rate of 10 °C per min, and the signals of NO (m/z=30), $N_2O$ (m/z=44), $NO_2$ (m/z=46); CO (m/z=28), $CO_2$ (m/z=44), $H_2$ (m/z=2); and SO (m/z=48) were monitored.

(9) In situ diffuse reflectance infrared Fourier transform spectroscopy (In-situ DRIFTS)

In–situ DRIFTS data was collected using a Thermo Fisher (Nicolet 6700) Fourier transform infrared spectrometer equipped with liquid nitrogen–cooled MCT detector. All spectra were obtained with a resolution of 4 $cm^{-1}$, and each spectrum was generated from 16 scans. A background correction was applied to each spectrum.

## 3. Results and discussion

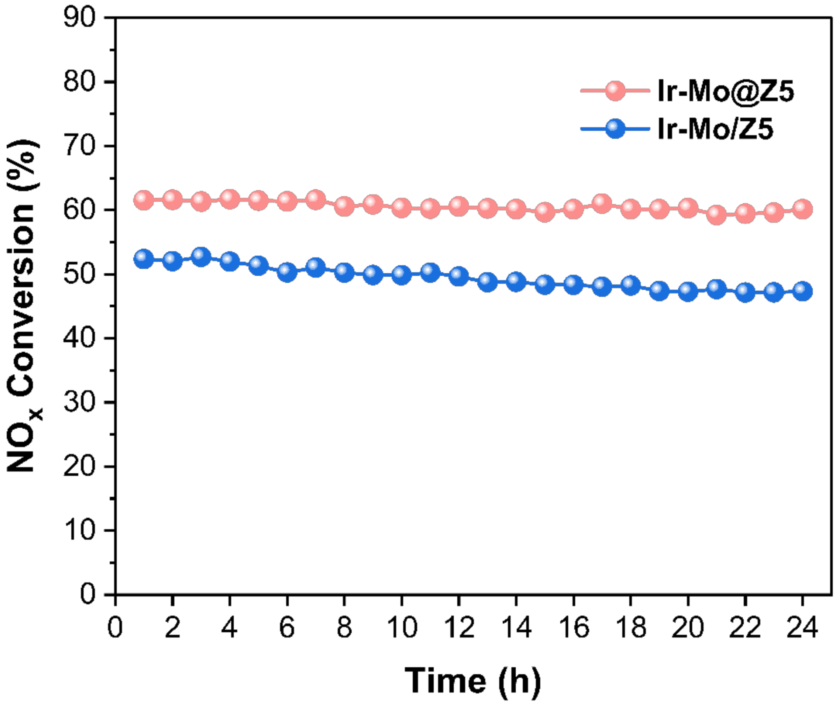

**Supplementary Figure 2. NO$_x$ conversion of Ir–Mo@Z5 and Ir–Mo/Z5 in the long-term stability test. Reaction conditions: [NO] = 400 ppm, [CO] = 8000 ppm, [O$_2$] = 5%, GHSV = 16000 h$^{-1}$.**

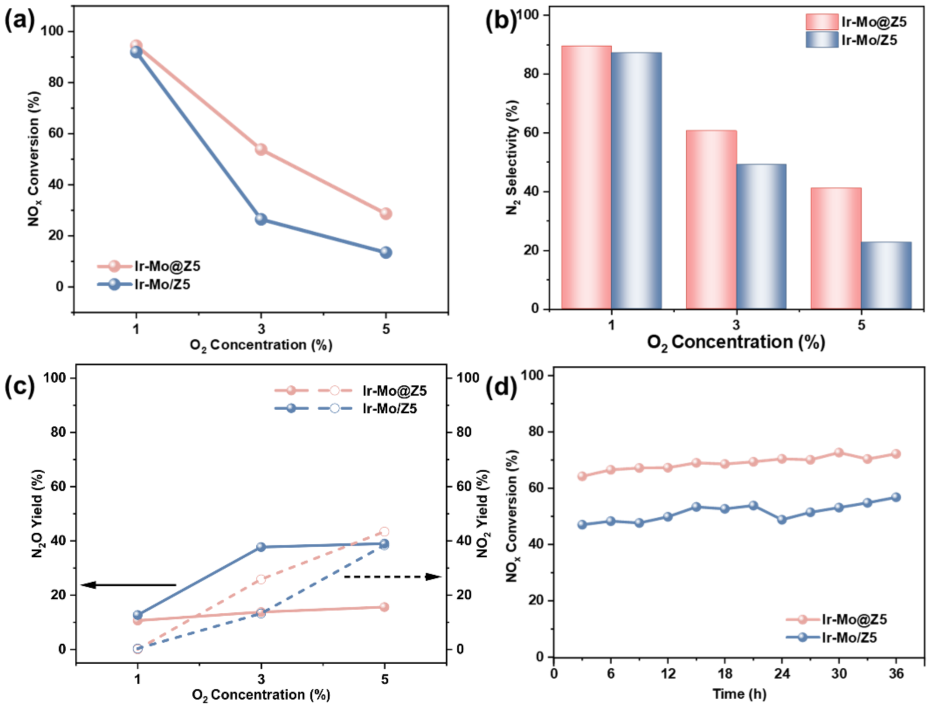

**Supplementary Figure 3. CO-SCR activity on catalysts under different $O_2$ concentrations: (a) NO conversion, (b) $NO_x$ conversion, (c) CO conversion, (d) $N_2$ selectivity. Reaction conditions: [NO] = 400 ppm, [CO] = 8000 ppm, [$O_2$] = 1-5%, GHSV = 16000 $h^{-1}$, 275 °C.**

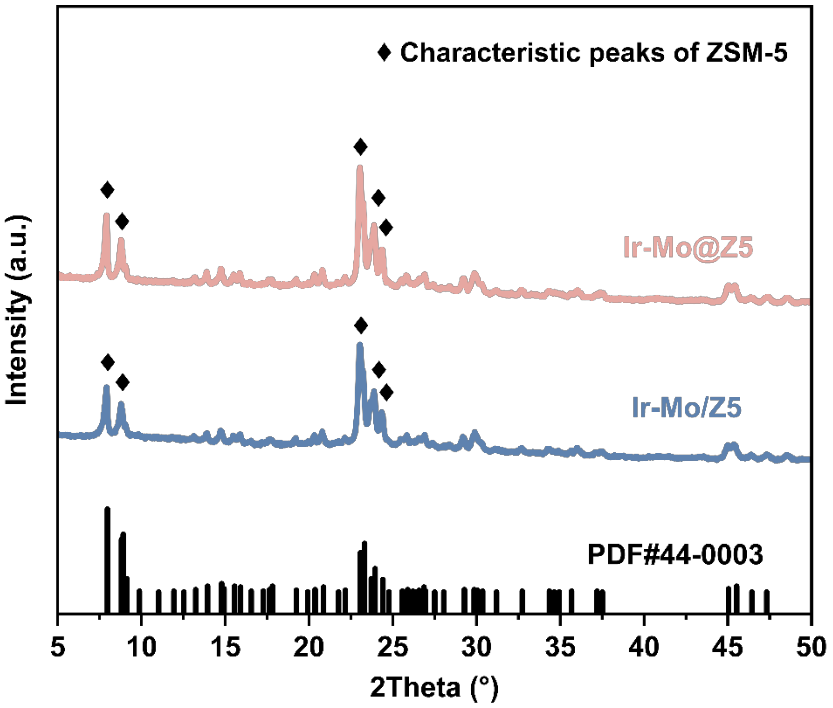

**Supplementary Figure 4. XRD patterns of all the catalysts. XRD: X-ray diffraction.**

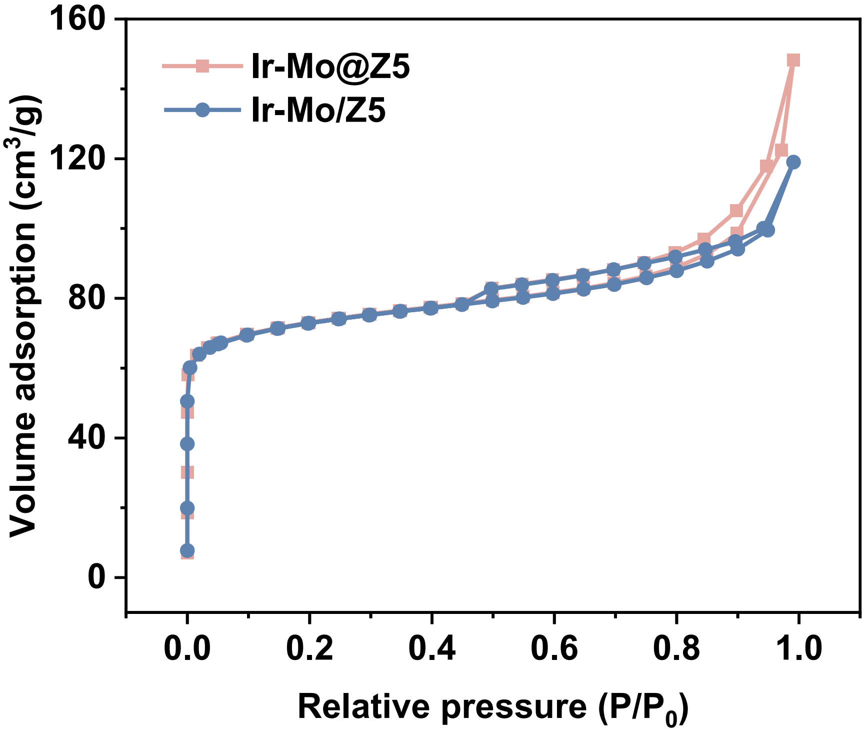

**Supplementary Figure 5. $N_2$ adsorption-desorption isotherms of the catalysts.**

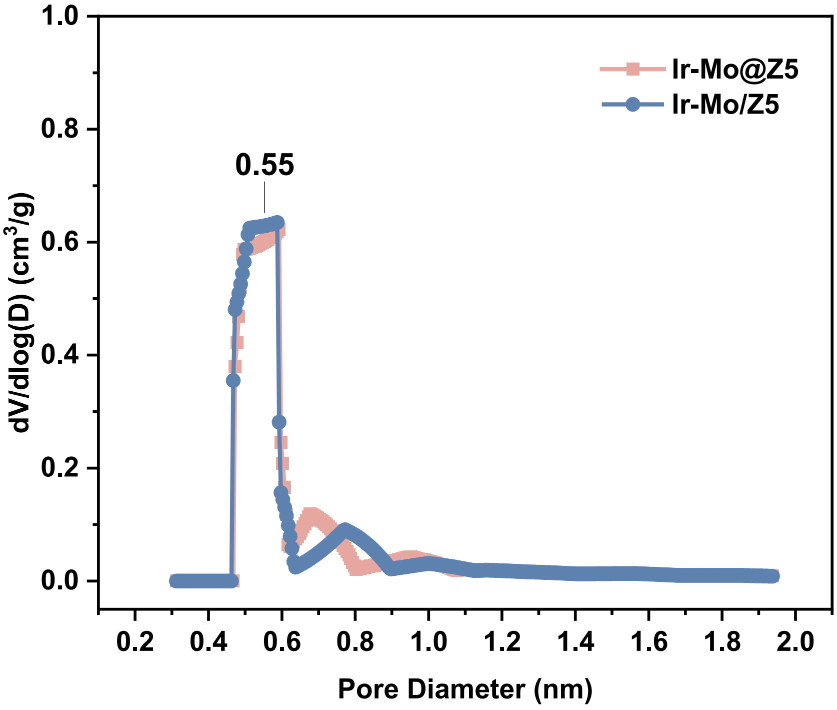

**Supplementary Figure 6. Pore-size distribution for catalysts.**

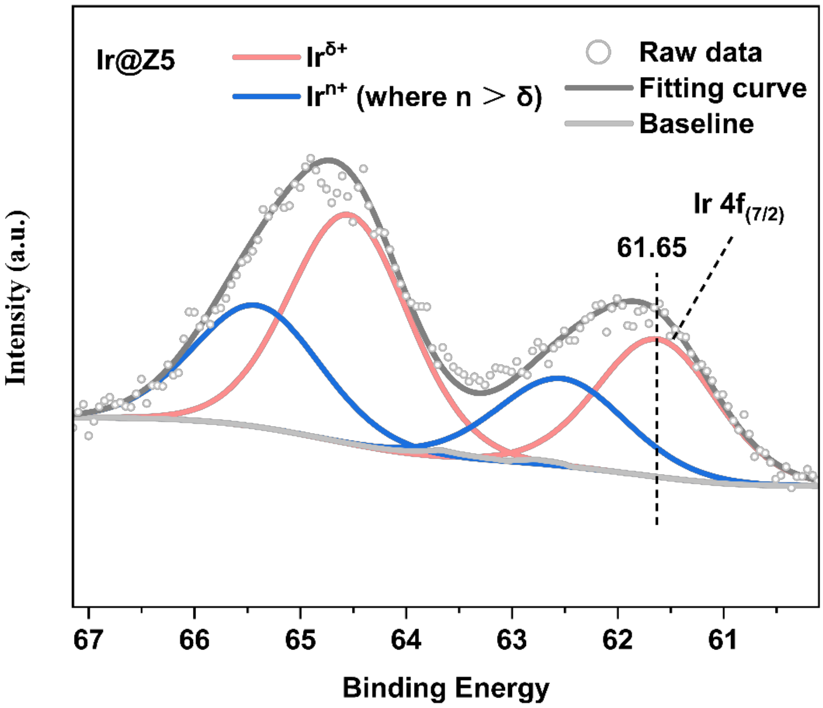

**Supplementary Figure 7. Ir 4f XPS spectra of Ir@Z5 catalysts.**

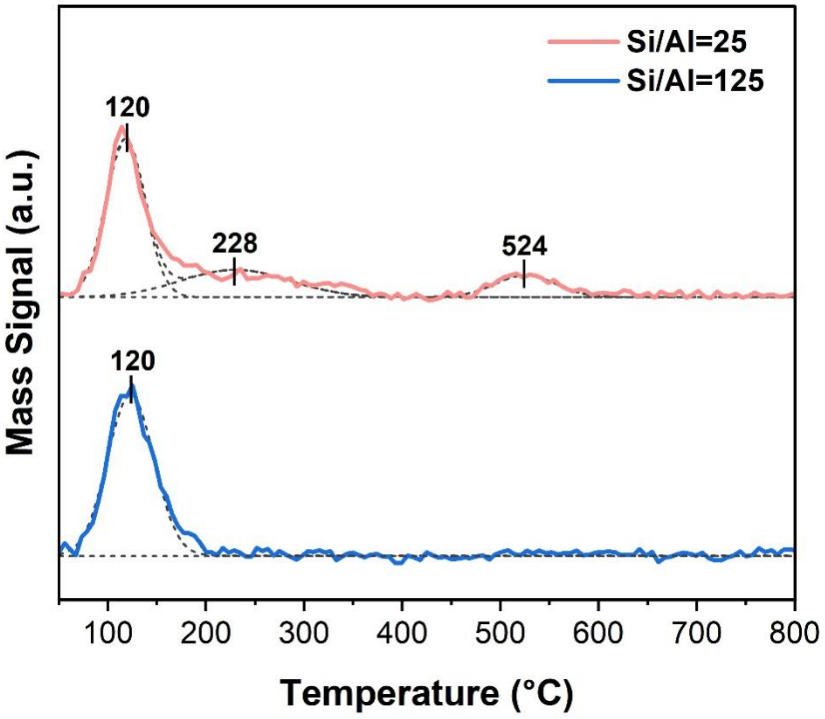

**Supplementary Figure 8. $SO_2$–TPD profiles of Z5 supports with different Si/Al.**

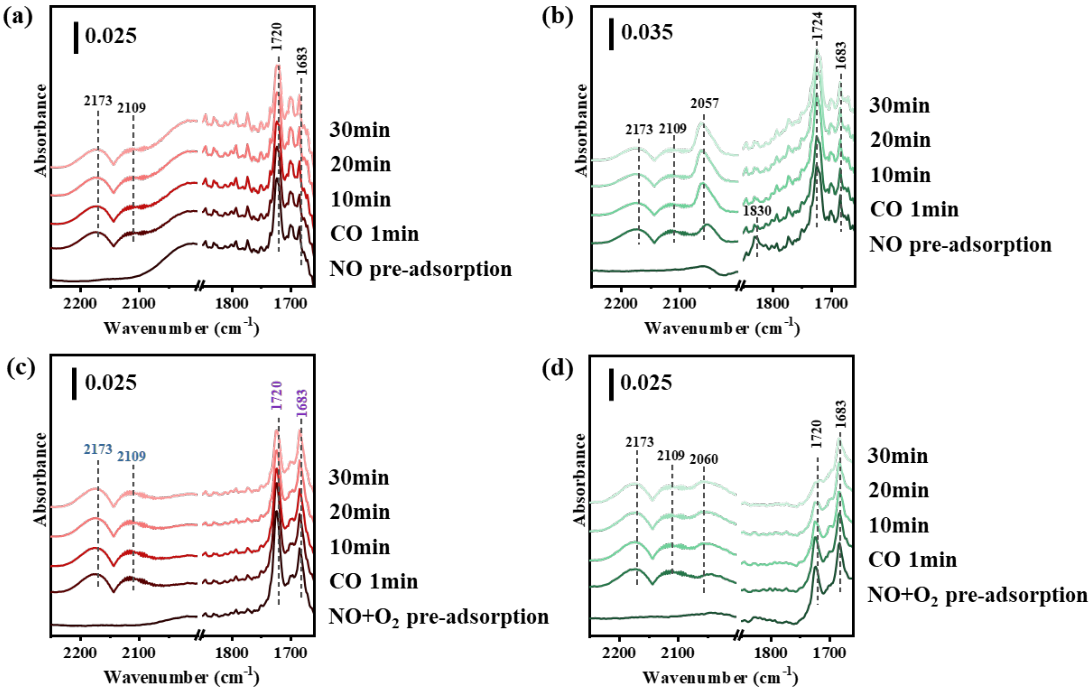

**Supplementary Figure 9. In-situ DRIFTS spectra of Ir-Mo@Z5 (a, c) and Ir-Mo/Z5 (b, d) catalysts at 275 °C: (a, b) Reaction between CO and pre-adsorbed NO; (c, d) Reaction between CO and pre-adsorbed NO + $O_2$. Reaction conditions: [NO] = 400 ppm, [CO] = 8000 ppm, [$O_2$] = 3% (when needed), and Ar as balance gas.**

**Supplementary Table 1. Comparison of CO-SCR performance between Ir-Mo@Z5 and other bimetallic catalysts.**

| Catalyst | Main metal loading (wt. %) | Reaction condition |  |  |  | $NO/NO_x$ conversion (%) | Temperature (°C) | Ref. |
|---|---|---|---|---|---|---|---|---|
|  |  | NO ppm | CO ppm | $O_2$ (%) | GHSV or WHSV |  |  |  |
| Ir-Mo@Z5 | 0.35 | 400 | 8000 | 5 | 16000 $h^{-1}$ | 84 | 275 | This work |
| IrW-$WO_3$/KIT-6 | 1.0 | 1000 | 4000 | 5 | 50000 $h^{-1}$ | 54 | 250 | 1 |
| Ir/$WO_3$-$SiO_2$ | 1.0 | 500 | 5000 | 5 | 20000 $h^{-1}$ | ~50 | 270 | 2 |
| IrRu/ZSM-5 | 0.5 | 50 | 6000 | 5 | 100000 $h^{-1}$ | ~80 | 275 | 3 |
| IrRu/$Al_2O_3$ | 1.9 | 50 | 7000 | 5 | 120000 mL $g^{-1}$ $h^{-1}$ | ~52 | 250 | 4 |
| Pt-CuO/CuAlO | 0.02 | 1000 | 2000 | 3 | 10000 $h^{-1}$ | 70 | 250 | 5 |

**Supplementary Table 2. Structural parameters of the synthesized catalysts.**

| Catalyst | $S_{BET}$ ($m^2g^{-1}$) | $V_p$ ($cm^3g^{-1}$) | Ir loading (wt.%) | Mo loading (wt.%) | Si/Al |
|---|---|---|---|---|---|
| Ir-Mo@Z5 | 279.12 | 0.13 | 0.35 | 0.85 | 24.68 |
| Ir-Mo/Z5 | 278.10 | 0.08 | 0.46 | 0.83 | 24.35 |

## References

[1] Ji Y.J.; Liu S.M.; Zhu H.D.; Xu W.Q.; Jiang R.H.; Zhang Y.; Yu J.; Chen W.X.; Jia L.H.; Jiang J.G.; Zhu T.Y.; Zhong Z.Y.; Wang D.S.; Xu G.W.; Su F.B. Isolating contiguous Ir atoms and forming Ir-W intermetallics with negatively charged Ir for efficient NO reduction by CO. Adv. Mater. **2022**, 34, 2205703. DOI: 10.1002/adma.202205703

[2] Wang J.Y.; Gao F.Y.; Yi H.H.; Liu H.H.; Xiong T.K.; Du Y.; Zhou Y.S.; Duan E.H.; Tang X.L. Strong Ir-W interaction boosts CO-SCR denitration over supported Ir-based catalysts and influential mechanism of oxygen. Sep. Purif. Technol. **2023**, 325, 124684. DOI: 10.1016/j.seppur.2023.124684

[3] Bai Y.R.; Gao S.; Sun Y.X.; Ouyang W.L.; Zhou Y.; Wang H.Q.; Wu Z.B. Insight into the mechanism of selective catalytic reduction of NO by CO over a bimetallic IrRu/ZSM-5 catalyst in the absence/presence of $O_2$ by isotopic $C^{13}O$ tracing methods. Environ. Sci. Technol. **2023**, 57, 9105–9114. DOI: 10.1021/acs.est.3c01640

[4] Song, J.H.; Park, D.C.; You, Y.W.; Kim, Y.J.; Lee, J.H.; Heo, I.; Kim, D.H. Promotive effects of Ba addition on lean $NO_x$ reduction by CO over IrRu/$Al_2O_3$ catalyst. Chem. Eng. J. **2022**, 452, 139331. DOI: 10.1016/j.cej.2022.139331

[5] Ji Y.J.; Liu S.M.; Song S.J.; Xu W.Q.; Li L.; Zhang Y.; Chen W.X.; Li H.F.; Jiang J.G.; Zhu T.Y.; Li Z.X.; Zhong Z.Y.; Wang D.S.; Xu G.W.; Su F.B. Negatively Charged Single-Atom Pt Catalyst Shows Superior SO2 Tolerance in NOx Reduction by CO. ACS Catal. **2023**, 13, 224-236. DOI: 10.1021/acscatal.2c04918